ChemComm

The Electroneutrality Condition Allows for Electrodeposition of Gold Nanoparticles from Aqueous Nanodroplets

Journal:	*ChemComm*
Manuscript ID	CC-COM-06-2022-003645.R1
Article Type:	Communication

ARTICLE

The Electroneutrality Condition Allows for Electrodeposition of Gold Nanoparticles from Aqueous Nanodroplets

Received 00th January 20xx,
Accepted 00th January 20xx

DOI: 10.1039/x0xx00000x

Joshua Reyes-Morales,[a] Mohamed Moazeb, [a] Guillermo S. Colón-Quintana,[a] and Jeffrey E. Dick [a,b*]

Nanodroplet-mediated electrodeposition is a reliable method for electrodepositing nanoparticles by confining a small amount of metal-salt precursor in water nanodroplets (radius ~400 nm) suspended in an oil continuous phase. This technique provides a great advantage in terms of nanoparticle size, morphology, and porosity. For an electrochemical reaction to proceed in the aqueous nanodroplet, the electroneutrality condition must be maintained. Classically, $[NB_4][ClO_4]$ or a comparable salt is added to the oil continuous phase to maintain charge balance. Unfortunately, the presence of this salt in the oil phase causes some metal salts, such as $HAuCl_4$, to phase transfer, disallowing the formation of gold nanoparticles. Here, we demonstrate the partitioning of $HAuCl_4$ is orders of magnitude lower using Inductively Coupled Plasma Mass Spectrometry (ICP-MS) when $LiClO_4$ is added to the nanodroplet phase and $[NBu_4][ClO_4]$ is not added to the continuous phase. This simple change allows for the electrodeposition of gold nanoparticles. Scanning electron microscopy shows the morphology and size distribution of gold nanoparticles obtained at different concentrations of $LiClO_4$. Transmission electron microscopy in selected diffraction mode was used and it determined the gold nanoparticles obtained are polycrystalline with miller indices of (222) and (200). This work widens the variety of nanoparticles that can be electrodeposited from nanodroplets for applications in energy storage and conversion, photoelectrochemistry, and biosensing.

Introduction

Historically, nanoparticle electrosynthesis has been a method of for the generation of different materials that can be applied to nanotechnology, biology, energy, separations, etc.[1, 2] A recently developed technique for nanoparticle electrosynthesis, called nanodroplet-mediated electrodeposition, uses a small amount of a metal-salt precursor confined within water nanodroplets that are suspended in an organic phase that contains supporting electrolyte. [3-5] During this process, when a potential is applied using a 3-electrode system, the metal salt precursor can be reduced at the water-electrode interface to generate nanoparticles. Multiple groups have taken advantage of this method to generate different metal and non-metal nanoparticles.[6-8] Various nanoparticles have been electrodeposited with this technique, including Pt nanoparticles,[4, 9] high entropy alloys,[10, 11] etc.

For nanodroplet mediated electrodeposition, the selection of the metal-salt precursor and supporting electrolyte is extremely important. When metal salts are reduced in the water nanodroplet, electroneutrality must be maintained. Historically, tetrabutylammonium perchlorate ($[NBu_4][ClO_4]$) has been used in the oil continuous phase.[12-14] During the reduction of the metal salt, NBu_4^+ transfers across the liquid|liquid interface to maintain electroneutrality. Unfortunately, NBu_4^+ is a phase transfer catalyst and spontaneously causes some metal salt precursors, such as $HAuCl_4$, to transfer into the oil continuous phase.[15, 16] Consequently, the electrodeposition of the metal also takes place in the oil phase, resulting in it being difficult to confine the reaction to the water droplets. We recently showed that one can exclude $[NBu_4][ClO_4]$ in the oil phase and add

[a] Department of Chemistry, The University of North Carolina at Chapel Hill, Chapel Hill, NC 27599, USA

*Corresponding author: jedick@email.unc.edu

b Lineberger Comprehensive Cancer Center, School of Medicine, The University of North Carolina at Chapel Hill, Chapel Hill, NC 27599, USA

Electronic Supplementary Information (ESI) available. See DOI: 10.1039/x0xx00000x

$LiClO_4$ to the water nanodroplet phase.[3] In general, the method can be extended to the electro-reduction of other metal salts, such as chloroplatinate.[3] This simple change drives down the experimental cost of nanodroplet mediated electrodeposition by orders of magnitude. Previously, our group electrodeposited high entropy alloys.[10] Metals like gold was not included due to the partitioning of $HAuCl_4$ into the 1,2-dichloroethane phase. In this article, experimental data is provided to demonstrate that $HAuCl_4$ will transfer into a dichloroethane continuous phase in the presence of $[NBu_4][ClO_4]$. When $HAuCl_4$ is dissolved in the water nanodroplet in the presence of $LiClO_4$, phase transfer does not occur, allowing for the electrodeposition of gold nanoparticles. Electroneutrality is maintained during the electro-reduction of $AuCl_4^-$ by the transfer of ClO_4^- from the water nanodroplet phase to the dichloroethane continuous phase. Our experiments expand the library of metals that can be synthesized using nanodroplet mediated electrodeposition.

Results and discussion

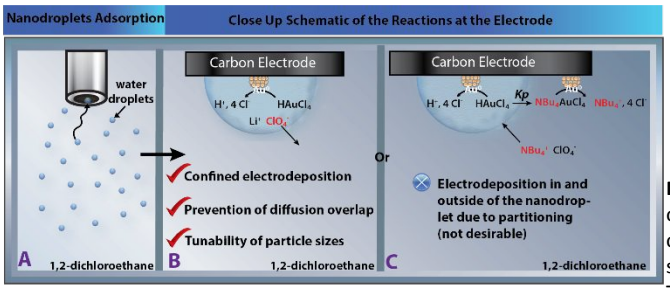

Figure 1. Schematic representation of the electrodeposition of gold nanoparticles using a quiescent solution. a) Representation of water nanodroplets suspended in an organic phase where they adsorb into the electrode surface. b) In the presence of $LiClO_4$, the redox reaction is confined at the water-electrode interface while c) in the presence of $[NBu_4][ClO_4]$, the reaction happens both inside and outside the water nanodroplet.

Electrodeposition of several metals using the nanodroplet-mediated process is possible.[7, 11, 17, 18] For a general representation, usually, these systems have water nanodroplets containing a metal-salt precursor suspended in an organic phase. The reason behind using a water-in-oil system is because that most of the metal-salt precursors are water soluble.[19-21] For the experiments shown, the system used is water nanodroplets suspended in a 1,2-dichloroethane phase where the water nanodroplets contain a metal-salt precursor. With time, these nanodroplets collide stochastically at the electrode surface (**Figure 1a**). Depending on which phase the supporting electrolyte is added to, the charge balance mechanism will change.[3, 12, 22-25] By adding the supporting electrolyte in the water phase, such as $LiClO_4$, when a high cathodic potential is applied the $AuCl_4^-$ is reduced to generate gold nanoparticles (**Figure 1b**); to maintain charge balance, ClO_4^- leaves the water nanodroplet, as dictated by the Gibbs free energy.[14, 25] $LiClO_4$ was chosen since it is not electrochemically active at the potentials used, it does not precipitate in the presence of the metal salts chosen, and the facilitated ion transfer of the perchlorate anion into the 1,2-dichloroethane phase upon the reduction of the metal-salt precursor is favored to maintain electroneutrality.[14, 26] Salts like KCl are difficult for these experiments since the Cl^- anion is significantly hydrophilic; therefore, the reduction of metal salts would be thermodynamically unfavorable resulting in applying a higher cathodic overpotential.[26, 27] The use of other salts in the water phase for gold electrodeposition will be a topic of future interest. However, when $[NBu_4][ClO_4]$ is added into the 1,2-dichloroethane, the partitioning of $HAuCl_4$ happens between the water and the 1,2-dichloroethane, leading to the electrodeposition of gold nanoparticles at the water-electrode and organic-electrode boundaries (**Figure 1c**). Electrogeneration of nanoparticles at both interfaces (i.e., water-electrode and organic-electrode) is not desirable because it won't be possible to have control over the synthesis of gold nanoparticles, in this case.

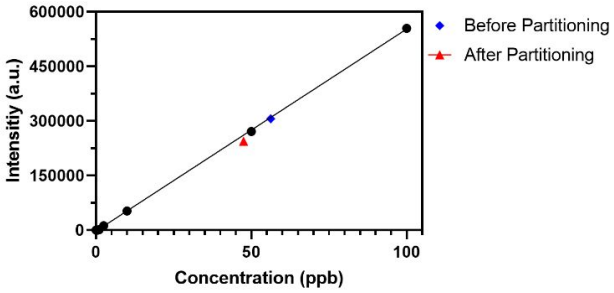

Figure 2. Calibration curve for the determination of the partition coefficient of $HAuCl_4$ using ICP-MS. Gold standards of known concentration were used and diluted by the instrument, with all samples being diluted with 2% HNO_3 prior to measurement on ICP-MS. The gold standard concentrations were 100, 50, 10, 1, and 0 ppb. Concentrations for standards shown are plotted against raw intensity counts and have arbitrary units (a.u.). All calibration curve measurements were taken at an N=5, with measurements for 2.5 mM $HAuCl_4$ with 0.1 M $LiClO_4$ in water partitioning being taken before and after mixing with 1,2-dichloroethane (N=10).

Partition coefficients for $HAuCl_4$ were obtained using inductive coupled plasma mass spectrometry (ICP-MS). Measurements for a 2.5 mM $HAuCl_4$ with 0.1 M $LiClO_4$ in water were taken both before and after the addition of an equal volume of 1,2-dichloroethane, with vigorous shaking (5 minutes) taking place in between both measurements. The concentration of $HAuCl_4$ was then determined for each phase after mixing with an ICP-MS calibration curve shown in **Figure 2**. With the difference in concentration being attributed to partitioning of $HAuCl_4$ from the aqueous base solution to the organic solution. Error bars for points shown within graph were added but are too small to be perceived. The statistical data and error bar information can be seen in **Table S1**. To quantify the degree of partitioning, **Equation 1** was used, where in the ratio of concentration in the organic phase over the aqueous phase will provide a coefficient of portioning (K_p).

Eq. 1 $$HAuCl_{4\,Water} \overset{K_p}{\leftrightarrow} HAuCl_{4\,1,2-\text{dichloroethane}} ; K_p = \frac{[HAuCl_4]_{Water}}{[HAuCl_4]_{1,2-\text{dichloroethane}}}$$

Smaller partition coefficients indicate higher affinity towards the aqueous solutions and higher values indicating greater preference towards organics solutions such as 1,2-

dichloroethane. In the absence of $[NBu_4][ClO_4]$, $K_p = 0.155$ and in the presence of 0.1 M $[NBu_4][ClO_4]$, $K_p = 930$. Thus, $HAuCl_4$ is nearly 6,000 times more soluble in the 1,2-dichloroethane in the presence of $[NBu_4][ClO_4]$.

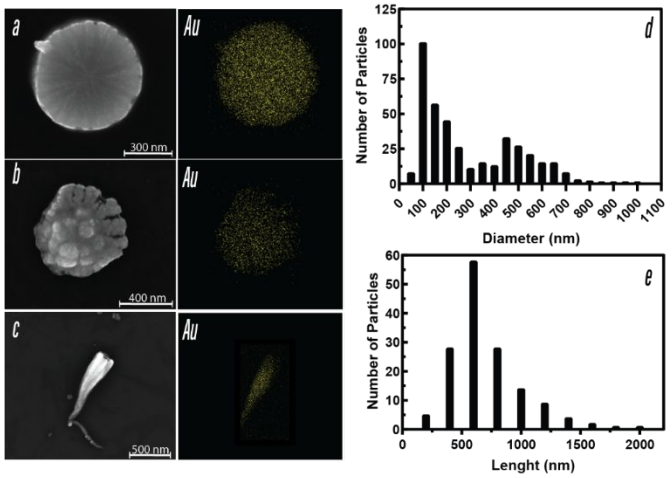

Figure 3. a, b, and c are SEM Images of representative gold nanoparticles (**left**) electrodeposited using a water-in-oil emulsion. The emulsion was prepared by adding 25 mM $HAuCl_4$ and 0.25 M $LiClO_4$ to water nanodroplets suspended in 1,2-dichloroethane. EDX mapping was performed showing the presence of gold across each nanoparticle (**yellow**). d) The histogram shows a relationship between the number of nanoparticles and size (N= 402) when the nanoparticles look more spherical as presented in a, and b. e) Histogram and SEM images of nanoparticles that are not spherical (N= 150) as presented in c. Nanoparticles were electrodeposited using chronoamperometry. The applied potential was – 0.1 V vs Ag/AgCl for 600 seconds. The average droplet radius was 1037 nm ± 238 nm (N=10).

Gold nanoparticles were electrodeposited on a highly oriented pyrolytic graphite (HOPG) using the nanodroplet system in the presence of $LiClO_4$ inside the water nanodroplets using chronoamperometry with a quiescent emulsion (**Figure S1**). The chronoamperogram showed in **Figure S1** does not follow the Cottrell equation due to the lack of electrolyte in the 1,2-dichloroethane phase resulting in a higher resistance, as we previously explained in our recent publication.[3] Electrodeposition was performed at a potential more negative than the formal potential (**Figure S5**) to make sure that gold nanoparticles could be obtained. Further negative potentials could lead to unfavorable reactions (e.g., ORR and HER) that could compete kinetically with the nucleation and growth of gold nanoparticles. Moreover, 600 seconds was picked to obtain a higher number of nanoparticles on the surface by providing more time for the stochastic collisions of the droplets to occur.[7, 14] **Figure 3** shows representative SEM and EDX mapping images of several gold nanoparticles. We observed that for 60% of the samples, the nanoparticles were spherical (**Figure 3a** and **3b**) and for 40% of the samples, the nanoparticles were non-spherical (**Figure 3c**). Moreover, **Figure 3d** shows the size distribution of the more spherical nanoparticles (as seen in **Figure 3a** and **3b**) to be 294 nm ± 197 nm in diameter when N= 402 nanoparticles. Non-spherical nanoparticles (as seen in **Figure 3c**) show an average of 710 nm ± 312 nm in diameter when N= 105 nanoparticles (**Figure 3e**). The difference in morphology will be the topic of a future investigation. In addition, the electrodeposition of gold nanoparticles was performed in the presence of different concentrations of $LiClO_4$ showing no significant changes in morphology (**Figure S7**). However, SEM images show that there is a difference in the nanoparticle coverage using different concentrations of $LiClO_4$ (**Figure S7a**). Interestingly, nanoparticles are obtained at a concentration as low as only 5 mM $LiClO_4$ but with a lower nanoparticle coverage. Since only 5 mM $LiClO_4$ is available, $HAuCl_4$ will not significantly electro-reduce. This observation implies that lower $LiClO_4$ concentrations favor electrodeposition from larger droplets. When no $LiClO_4$ was added to the aqueous phase, no nanoparticles are observed (**Figure S6**).

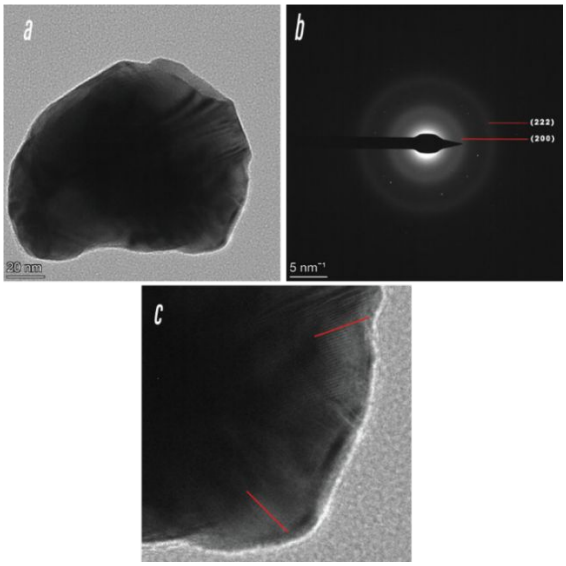

Figure 4. TEM images of a single gold nanoparticle. a) Shows a bright field image and b) shows the selected area diffraction pattern of the gold nanoparticle with their respective miller indices. Additionally, c) shows the lattice orientation.

Additionally, TEM images were obtained (**Figure 4a**). The rings and the small bright spots in the selected area electron diffraction (**Figure 4b**) indicates that gold nanoparticles are polycrystalline. Furthermore, **Figure 4c** shows the orientation of the lattices in the nanoparticle with the red lines indicating the direction of the crystal lattices. This clearly supports that the gold nanoparticles are polycrystalline. Moreover, the d-spacing values obtained from the diffractogram (**Table S2**) are in good agreement with the literature values; therefore, the crystal faces were determined to be (200) and (222) from **Figure 4b**.[28]

Conclusions

In conclusion, we have extended nanodroplet-mediated electrodeposition to metals that are susceptible to phase transfer. We achieved this by confining the metal salt in the nanodroplet with $LiClO_4$. ICP-MS supported the low partitioning of gold salts into the organic phase. SEM showed differences in morphology of nanoparticles. This system permits the generation of nanoparticles at a lower cost. Not only that, but we expanded the library of nanoparticles that can be electrodeposited by using the nanodroplet-mediated electrodeposition method.

Author Contributions

All authors have given approval to the final version of the manuscript.

Conflicts of interest

There are no conflicts to declare.

Acknowledgements

We acknowledge the support by the National Science Foundation CAREER under grant number CHE-2045672. We also acknowledge the use of scanning electron microscopy, and transmission electron microscopy instrumentation at the Chapel Hill Analytical and Nanofabrication Laboratory, CHANL, a member of the North Carolina Research Triangle Nanotechnology Network, RTNN, which is supported by the National Science Foundation, Grant ECCS-2025064, as part of the National Nanotechnology Coordinated Infrastructure, NNCI. We additionally acknowledge the use of inductive coupled plasma mass spectroscopy at the Nanomedicines Characterization Core Facility (NCore).

Notes and references

1. Khan, I.; Saeed, K.; Khan, I., Nanoparticles: Properties, applications and toxicities. *Arabian Journal of Chemistry* **2019,** *12* (7), 908-931.
2. Botteon, C. E. A.; Silva, L. B.; Ccana-Ccapatinta, G. V.; Silva, T. S.; Ambrosio, S. R.; Veneziani, R. C. S.; Bastos, J. K.; Marcato, P. D., Biosynthesis and characterization of gold nanoparticles using Brazilian red propolis and evaluation of its antimicrobial and anticancer activities. *Scientific Reports* **2021,** *11* (1), 1974.
3. Reyes-Morales, J.; Vanderkwaak, B. T.; Dick, J. E., Enabling practical nanoparticle electrodeposition from aqueous nanodroplets. *Nanoscale* **2022,** *14* (7), 2750-2757.
4. Glasscott, M. W.; Pendergast, A. D.; Dick, J. E., A Universal Platform for the Electrodeposition of Ligand-Free Metal Nanoparticles from a Water-in-Oil Emulsion System. *ACS Applied Nano Materials* **2018**.
5. Park, J. H.; Jin, S.-M.; Lee, E.; Ahn, H. S., Electrochemical synthesis of core–shell nanoparticles by seed-mediated selective deposition. *Chemical Science* **2021,** *12* (40), 13557-13563.
6. Saw, E. N.; Grasmik, V.; Rurainsky, C.; Epple, M.; Tschulik, K., Electrochemistry at single bimetallic nanoparticles – using nano impacts for sizing and compositional analysis of individual AgAu alloy nanoparticles. *Faraday Discussions* **2016,** *193* (0), 327-338.
7. Jeun, Y. E.; Baek, B.; Lee, M. W.; Ahn, H. S., Surfactant-free electrochemical synthesis of metallic nanoparticles via stochastic collisions of aqueous nanodroplet reactors. *Chemical Communications* **2018,** *54* (72), 10052-10055.
8. Lee, M. W.; Kwon, D.-J.; Park, J.; Pyun, J.-C.; Kim, Y.-J.; Ahn, H. S., Electropolymerization in a confined nanospace: synthesis of PEDOT nanoparticles in emulsion droplet reactors. *Chemical Communications* **2020,** *56* (67), 9624-9627.
9. Glasscott, M. W.; Dick, J. E., Fine-Tuning Porosity and Time-Resolved Observation of the Nucleation and Growth of Single Platinum Nanoparticles. *ACS Nano* **2019,** *13* (4), 4572-4581.
10. Glasscott, M. W.; Pendergast, A. D.; Goines, S.; Bishop, A. R.; Hoang, A. T.; Renault, C.; Dick, J. E., Electrosynthesis of high-entropy metallic glass nanoparticles for designer, multi-functional electrocatalysis. *Nature Communications* **2019,** *10* (1), 2650.
11. Percival, S. J.; Lu, P.; Lowry, D. R.; Nenoff, T. M., Electrodeposition of Complex High Entropy Oxides via Water Droplet Formation and Conversion to Crystalline Alloy Nanoparticles. *Langmuir* **2022,** *38* (5), 1923-1928.
12. Davies, T.; Wilkins, S.; Compton, R., The electrochemistry of redox systems within immobilised water droplets. *Journal of Electroanalytical Chemistry - J ELECTROANAL CHEM* **2006,** *586*, 260-275.
13. Zhang, H.; Sepunaru, L.; Sokolov, S. V.; Laborda, E.; Batchelor-McAuley, C.; Compton, R. G., Electrochemistry of single droplets of inverse (water-in-oil) emulsions. *Physical Chemistry Chemical Physics* **2017,** *19* (24), 15662-15666.
14. Terry Weatherly, C. K.; Glasscott, M. W.; Dick, J. E., Voltammetric Analysis of Redox Reactions and Ion Transfer in Water Microdroplets. *Langmuir* **2020,** *36* (28), 8231-8239.
15. Karmakar, R.; Samanta, A., Phase-Transfer Catalyst-Induced Changes in the Absorption and Fluorescence Behavior of Some Electron Donor−Acceptor Molecules. *Journal of the American Chemical Society* **2001,** *123* (16), 3809-3817.
16. Uchiyama, Y.; Tsuyumoto, I.; Kitamori, T.; Sawada, T., Observation of One Process in a Phase Transfer Catalytic Reaction at a Liquid/Liquid Interface by Using the Quasi-Elastic Laser Scattering Method. *The Journal of Physical Chemistry B* **1999,** *103* (22), 4663-4665.
17. Tarolla, N. E.; Voci, S.; Reyes-Morales, J.; Pendergast, A. D.; Dick, J. E., Electrodeposition of ligand-free copper nanoparticles from aqueous nanodroplets. *Journal of Materials Chemistry A* **2021,** *9* (35), 20048-20057.
18. Glasscott, M. W.; Dick, J. E., Direct Electrochemical Observation of Single Platinum Cluster Electrocatalysis on Ultramicroelectrodes. *Analytical Chemistry* **2018,** *90* (13), 7804-7808.
19. Schwämmlein, J. N.; Torres, P. A. L.; Gasteiger, H. A.; El-Sayed, H. A., Direct PtSn Alloy Formation by Pt Electrodeposition on Sn Surface. *Scientific Reports* **2020,** *10* (1), 59.
20. Ayyad, A. H.; Stettner, J.; Magnussen, O. M., Electrocompression of the Au(111) Surface Layer during Au Electrodeposition. *Physical Review Letters* **2005,** *94* (6), 066106.
21. Bonou, L.; Eyraud, M.; Denoyel, R.; Massiani, Y., Influence of additives on Cu electrodeposition mechanisms in acid solution: direct current study supported by non-electrochemical measurements. *Electrochimica Acta* **2002,** *47* (26), 4139-4148.
22. Terry Weatherly, C. K.; Ren, H.; Edwards, M. A.; Wang, L.; White, H. S., Coupled Electron- and Phase-Transfer Reactions at a Three-Phase Interface. *Journal of the American Chemical Society* **2019,** *141* (45), 18091-18098.
23. Tasakorn, P.; Chen, J.; Aoki, K., Voltammetry of a single oil droplet on a large electrode. *Journal of Electroanalytical Chemistry* **2002,** *533* (1), 119-126.
24. Moon, H.; Park, J. H., In Situ Probing Liquid/Liquid Interfacial Kinetics through Single Nanodroplet Electrochemistry. *Analytical Chemistry* **2021,** *93* (50), 16915-16921.
25. Osakai, T.; Naito, Y.; Eda, K.; Yamamoto, M., Prediction of the Standard Gibbs Energy of Transfer of Organic Ions Across the Interface between Two Immiscible Liquids. *The Journal of Physical Chemistry B* **2015,** *119* (41), 13167-13176.
26. Glikberg, S.; Marcus, Y., Relation of the Gibbs free energy of transfer of ions from water to polar solvents to the properties of the solvents and the ions. *Journal of Solution Chemistry* **1983,** *12* (4), 255-270.
27. Osakai, T.; Ebina, K., Non-Bornian Theory of the Gibbs Energy of Ion Transfer between Two Immiscible Liquids. *The Journal of Physical Chemistry B* **1998,** *102* (29), 5691-5698.
28. Ogundare, O. D.; Akinribide, O. J.; Adetunji, A. R.; Adeoye, M. O.; Olubambi, P. A., Crystallite size determination of thermally deposited Gold Nanoparticles. *Procedia Manufacturing* **2019,** *30*, 173-179.

